



# Ground Test Development of 800 lbf Nitrous Oxide-Ethane Engine

McKynzie J. Perry<sup>1</sup>, Aaron Hunt<sup>2</sup>, and Spencer Christian<sup>3</sup>  
*The University of Alabama in Huntsville, Huntsville, Alabama, 35805, United States*

**The Tartarus project has recently focused development efforts to the system to static fire its 800lbf Nitrous Oxide-Ethane rocket engine. This engine and ground system will be used with the Tartarus launch vehicle to reach a target altitude 30,000ft. The development of the static firing system has progressed counterintuitively, moving away from a more flight-like design in favor of higher safety factors and increased reliability. This paper details the deltas between the 2018 baseline flight-like system and the 2020 ground test system along with lessons learned during development.**

## I. Introduction

The Tartarus project is a liquid propulsion project at the University of Alabama in Huntsville within the Space Hardware Club. The team is led by and primarily composed of undergraduate students. The goal of the project is to design and fly a bipropellant rocket to 30,000 feet carrying a 9lb payload. The Tartarus project has been working towards the inaugural static fire of its 810lb nitrous oxide-ethane engine since 2017, under different project titles such as Liquid Propulsion Project, Bipropellant Engine Development, and Spaceport America Cup team. Over the course of 3 years, the comprehensive flight system has been designed and modified to meet mission objectives and prepare for test campaigns. This development has not occurred linearly, but for clarity the 2018 test stand design and the current 2020 test stand will be compared. These designs represent two different approaches to subsystem testing. The 2018 test stand was designed to be as similar to the proposed launch stand as possible, to reduce additional hardware acquisition. The 2020 test stand has incorporated industry experience with test stand failures and mitigations and moved away from the modified launch stand approach. While vestiges of the launch stand remain on the test stand, it's solely due to their usefulness as structural members. The current test stand is better equipped for the uncertainty inherent to early engine development testing.

## II. Preliminary Test Stand Design

Preliminary development for the propulsion and ground systems focused on the flight vehicle. The targeted flight date was in June 2018, 9 months after project kickoff, with a static fire targeted for early March. This static firing would have utilized as many potential flight systems as feasible, including in-house developed propellant tanks and valve actuators. The engine itself was a workhorse test article, thicker than its flight weight counterpart but utilizing the same injector design. The test stand would be the modified launch stand, with additional structure to hold the test article in place. This architecture for testing would have proven the stage rather than just the workhorse engine.

### A. Ground System Design

The PDR level ground system design consisted of 4 primary areas: the test stand, the fuel farm, the oxidizer farm, and the ground station. The test stand, fuel farm, and oxidizer farm were arranged in a triangle with 30 feet between each area. A render of the field is shown in Fig. 1.

---

<sup>1</sup> Undergraduate, Mechanical and Aerospace Engineering Department, [mp0062@uah.edu](mailto:mp0062@uah.edu), AIAA Student Member

<sup>2</sup> Undergraduate, Mechanical and Aerospace Engineering Department, [amh0070@uah.edu](mailto:amh0070@uah.edu), AIAA Student Member

<sup>3</sup> Undergraduate, Mechanical and Aerospace Engineering Department, [sc0169@uah.edu](mailto:sc0169@uah.edu), AIAA Student Member

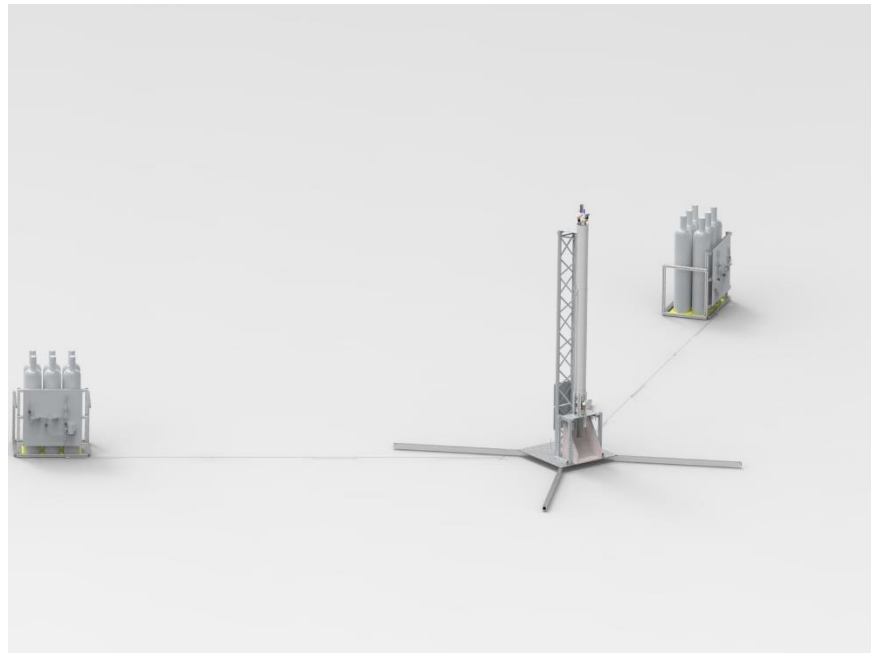


**Fig. 1 Render of Field Layout with Test Structures**

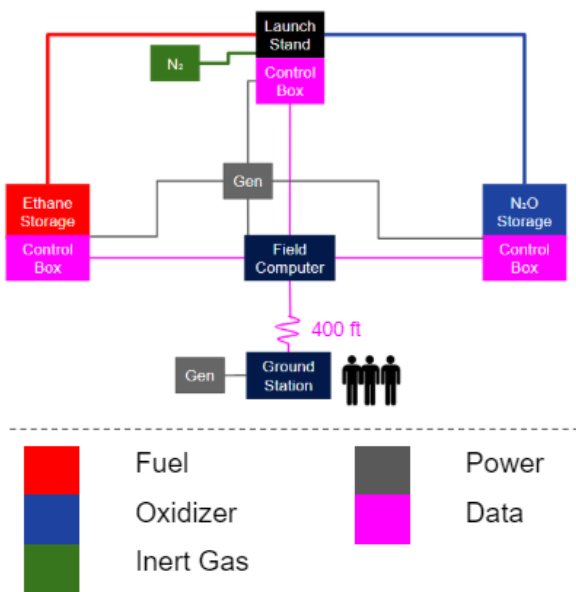


**Fig. 2 Block Diagram of Preliminary Ground System**

The computer system running command and control software was stationed in the center of the triangle, with a fiber optic communications cable running back to the ground station computers. A National Instruments USB-6210 DAQ was placed at each propellant farm and the test stand and would handle all instrument readings and valve commands for its respective area. The valves would be commanded through an Arduino, which would be directly sent a heartbeat signal from the main computer in addition to any commands from the DAQ. In the event the heartbeat signal is not detected, the Arduino would be able to independently safe the valves. A block diagram of the ground station is shown in

The test stand interfaced with the test article via 1515 t-slotted rail that was intended for launch. The propellant tanks were outfitted with rail guides to slide along the rail. This rail was supported by a 10ft F33 triangular truss, rated for up to a 682 pound load. Only the lower 10ft of the 30ft launch rail would be used, as that was all that was needed to support the static propellant tanks. At the bottom of the truss, a flame bucket made of sheet steel covered in refractory cement was attached to the baseplate to deflect the exhaust away from the test stand. To prevent the test article from lifting off, a hold down was developed using

aluminum square tubing and an aluminum plate. The plate would rest against the top of the engine with cut outs for the feed system. While holding the article at the top of the propellant tanks would be a more rigorous test of the structural integrity of the system, the materials required to produce a rigid hold down with the proper safety factors would have been significantly more expensive. Additionally, isolating the load of the engine below the hold down plate protected the rest of the fluid system from damage in the event of an engine anomaly. Creating a hold down attached to the base plate of the launch stand was more feasible and maintained the integrity of the stand for future launches. A render of the test stand from the right-side view is shown in Fig. 3.

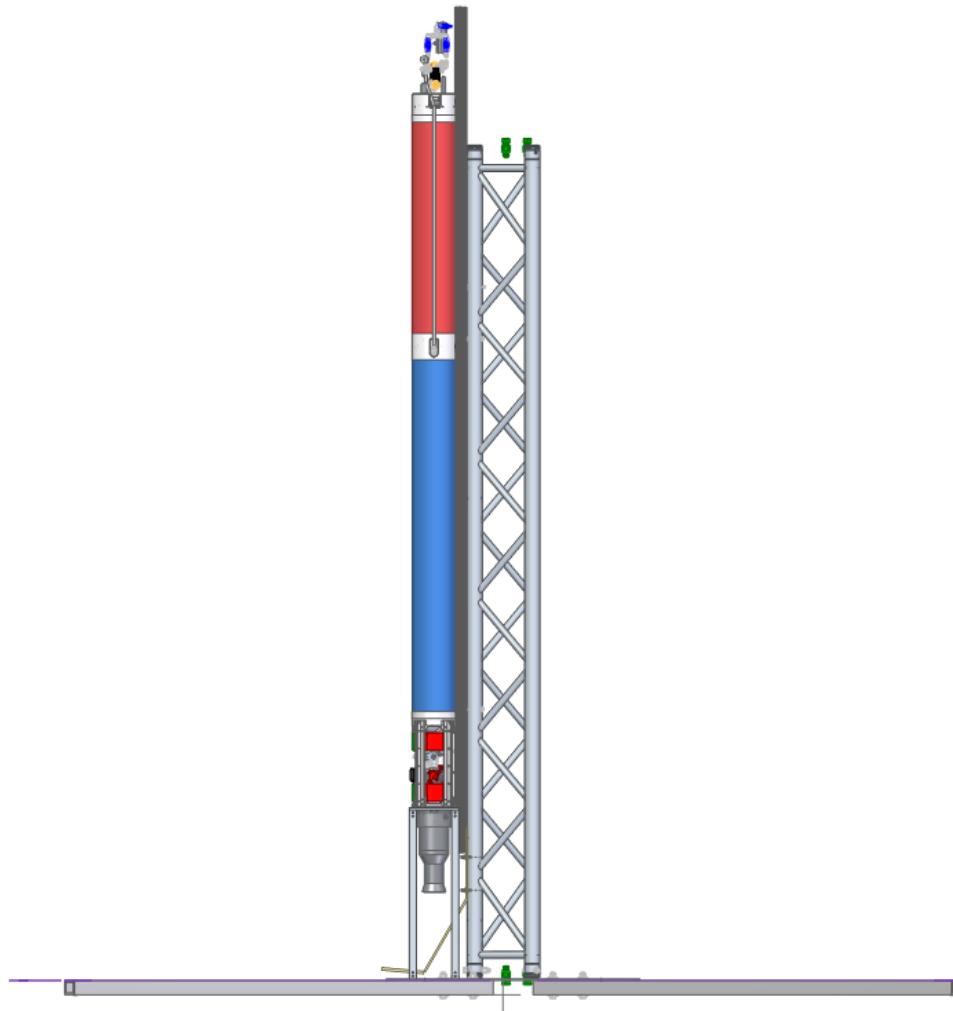


**Fig. 3 Render of Preliminary Test Stand with Test Article**

## **B. Test Article Development**

From an early point on the project, a choice was made to focus on flight systems. This precluded the development of much battleship or workhorse hardware, with the rationale that the cost reduction from avoiding hardware that would not directly flow into the final vehicle outweighed the potential risks of flight-weight testing campaigns. The first iteration engine was designed to be a workhorse, with additional material to withstand unexpected stresses. However, it was designed such that the additional material could easily be machined away later if the engine needed to become flight weight.

The workhorse engine itself was comprised of the fuel injector plate, fuel manifold cap, oxidizer injector element, and chamber/nozzle assembly, shown in Fig. 4. The fuel faceplate had 3 concentric zones of injection. A cross section of the fuel injector faceplate is shown in Fig. 5. The main combustion zone, Zone 1 (red), impinged upon the central oxidizer flow with an O/F ratio of 7. Zone 2 increased the ratio of fuel around the core combustion to bring down the O/F ratio to 3. Zone 3 (green) was strictly for film cooling the side walls of the engine. Due to the novelty of the cavitating venturi oxidizer injector element, the team wanted the capability to easily change oxidizer elements during test campaigns. This, and manufacturing complexity, drove the decision to not integrate the fuel and oxidizer injector designs into a single machined piece.

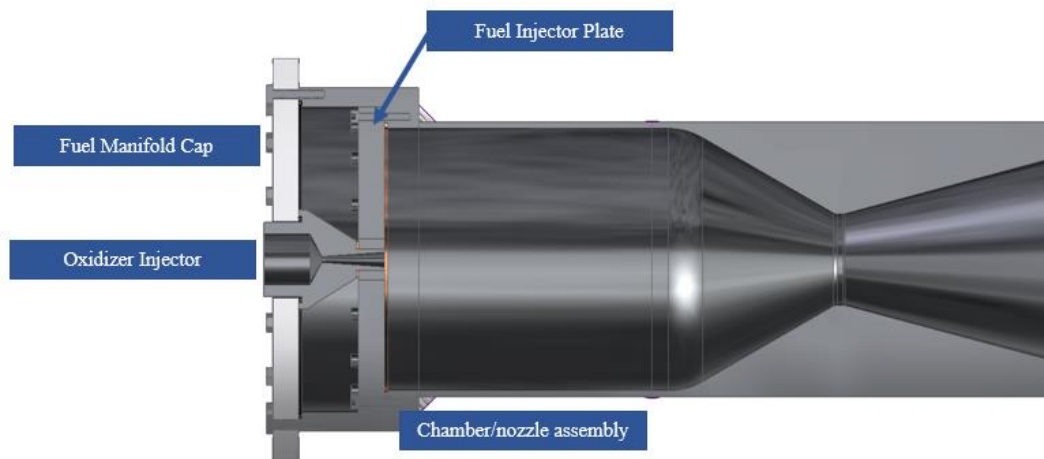


**Fig. 4 Preliminary Engine Render with Labels**



**Fig. 5 Fuel Injector Faceplate with Injection Zones**

There were 4 seals in this engine design. The fuel manifold cap was sealed against the oxidizer injector and chamber/nozzle assembly using elastomer rings. For the higher heat seals between the fuel injector and the oxidizer injector and the fuel injector and the chamber/nozzle assembly, custom copper gaskets were used. However, it was revealed in a later design review that an incorrect assumption was made while calculating the crush force necessary to seal against the copper, and the actual crush force would be significantly higher than anticipated. Additionally, due to the higher pressure of the fuel manifold compared to the combustion chamber, the fuel injector/oxidizer injector seal would inevitably leak while in operation. This drove a redesign of the upper portion of the engine discussed in Section III.C.

The feed system to the engine was flight-like, with an in-house designed and manufactured aluminum propellant tank unit. These tanks were 12 feet tall and 6 inches in diameter and designed to interface with the airframe of the launch vehicle. A cross section of the tanks are shown in Fig. 6, with circumferential welds highlighted in yellow. The propellant tanks were designed to a MAWP of 1000 psia with designed burst pressure above 2000 psia. The walls of the tanks were 6061-T6 aluminum round tube, and the bulkheads were machined in-house out of 6061 aluminum. The welding was contracted out and used 4043 filler. An 8 hour artificial aging at 350 °F was performed on the tanks to restore the heat affected zones of the welds to T6 temper. Prior to the engine firing, the tanks were hydrostatically pressure to 1.5x MAWP, 1500 psia. This test ended in failure, which is discussed in Section V.C.



**Fig. 6 Cross Section of Propellant Tanks**

Due to budget and size constraints, the trade space for flight valves was severely limited. Manual ball valves modified with servo actuators were selected for further development. A large concern of this design was the safing of the system in the event of communications loss. For this reason, servos with onboard PLC's were selected. If the servos lost connection to the command and control system they would return to a pre-programmed position. A render of the the servo and the ball valve with 4 bar linkage next to the development hardware is shown in Figure Fig. 7.

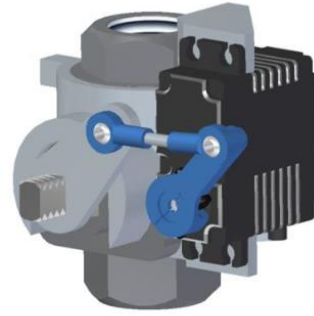


**Fig. 7 Render and Development Hardware of Servo-Driven Ball Valve**

Unfortunately, there were many issues with this design. The mount holding the ball valve to the actuating servo had more flexion than anticipated. This inefficiency reduced the effectiveness of the servo torque to the point where the ball valve would not open. Both direct linkage (by mounting the servo above the valve) and a gearing system were developed to solve the rigidity issues, but the opening time of the valve was incredibly slow, on the order of 4 seconds. This duration was not acceptable for the first engine firing tests, where quick valve response was critical. Additionally, the logic onboard the servo would detect the opening resistance from the valve as a failure, triggering it to abort and return to its original position. While this design still shows some promise for flight weight valves, the timeline of the firing and the unreliability of the servo driven ball valves caused them to be removed from the test stand in favor of more robust valves. In the future, more powerful servos and a more rigid mounting structure should be implemented.

### III. Current Test Stand Design

Two main events drove the design changes to the test stand: the failed hydrostatic testing of the run tanks and the critical design review of the system. The failure of the flight-weight tanks allowed for the acquisition of smaller, DOT rated run tanks, which significantly reduced the hazard of the system. The critical design review offered guidance from industry professionals on portions of the system that were not suitable for repetitive ground testing, creating revisions that improved reliability.

#### A. Ground System Fluids

The main changes to convert the launch stand to a ground system were structural, leading to many flaws and inconveniences in the preliminary test stand fluid design. One of the primary issues was the lack of drain system, which was avoided with the assumption that propellant could boil off through the vents if the tanks needed to be emptied. However, the nature of engine testing drove a change to add a dedicated drain system to the run tanks, to reduce the time necessary to remove all propellants from the system. This is both a safety and an operational convenience feature. The propellant drains to large, flat basins on opposite sides of the test stand. The drain system ball valves are piloted from the same solenoid valve, such that a “drain” command drains both tanks simultaneously. This simplifies abort logic and reduces the likelihood of human error during a drain procedure.

Another large flaw in the preliminary design was the trickle purge/muscle pressure system. The muscle pressure ran at 100 psi and piloted all ground system ball valves. However, there was also a leg of the system that vented through an orifice, check valve, and into the tanks. The rationale was that the run valves on the stand could be commanded open during setup operations to trickle nitrogen through the tanks and engine and reduce the likelihood of contamination. However, the constant flow of nitrogen severely hindered the muscle pressure system. Upon commanding a single valve to activate, the muscle pressure would drop so low that any other activated valves on the test stand would close. Additionally, the muscle pressure was run from the propellant farms to the test stand via 1/8” polyethylene tubing, causing significant pressure drop across the 30ft line. This issue is remedied through the addition of a dedicated nitrogen bottle and hard 1/4” line to the test stand for muscle pressure. The trickle purge will still be run through polyethylene tubing from the original nitrogen bottles at each propellant supply to keep the propellant feed systems completely isolated.

Finally, the nitrogen ullage pressurization system had to be addressed. This system was originally supplied from a single bottle to both propellant run tanks, with a check valve on each side to prevent backflow of one propellant into another. This system was devised to reduce the number of connection points between the vehicle and launch stand. However, check valves are notoriously leaky and reliability is paramount to a ground test system. With the other changes being made to improve the robustness of the system, the nitrogen supplies were isolated and a bottle was placed at each propellant farm for independent pressurization. This eliminated the risk of interpropellant mixing at any point in the system besides the engine.

## B. Test Stand Structures

The test stand structure has been improved primarily at the hold down and the run tank interface. While analysis supported the strength of the original hold down, the manufactured article lacked rigidity and did not inspire confidence. The factor of safety was also only 1.85, which did not meet requirements. The hold down is a critical safety feature to protect both personnel and the rest of the system. It was redesigned with a minimum factor of safety of 3 and more fault tolerance, primarily through the use of bolt patterns rather than single fasteners. After analysis, the hold down is rated to handle over 1500 pounds without violating the safety factor. It's primarily constructed using low carbon steel angle iron. The new hold down is shown Fig. 8.



**Fig. 8 Photo of Hold Down Structure on Baseplate**

Aside from the hold down, the other main structural change to the test stand was the interface between the run tanks and the tests stand. The original interface was the launch rail. However, the new tanks were significantly smaller and would be mounted onto a panel side-by-side instead of stacked. To best reuse materials on the test stand, such as the triangular truss, a unistrut chassis was developed for the panel that allowed it to mount to the truss and not interfere with the hold down. This structure had to carry the weight of the fluid panel and align the outlet of the valves with the inlet of the engine. The assembled main test stand (without flame bucket) is shown in Fig. 9.



**Fig. 9 Photo of Main Test Stand Structure**

### C. Engine

The sealing issue on the engine discussed in section II.B led to the redesign of the entire upper portion of the engine. The redesign was not straightforward. At CDR, the nozzle/chamber assembly was already manufactured and welded, and the injectors were partially manufactured. The injector geometries were maintained, as they were not yet proven or failed and the team had already collected water flow data on the injector elements. The injector elements were combined into a single part injector to eliminate interpropellant seals. Due to its better thermal conductivity and manufacturability, 6061 aluminum was selected as the material for the new injector. The machining of the injector would be more involved with more setups, but the change from 316 stainless steel significantly improved the manufacturability, especially with the 0.018" holes in zone 2 and 3. Additionally, the modularity of the oxidizer injector was lost. However, modularity is the enemy of reliable sealing. The fuel manifold walls were also incorporated into the injector design, to eliminate the possibility of additional fuel leakage into the combustion chamber and allow for the use of larger fasteners. A render of the injector is shown in Fig. 10.

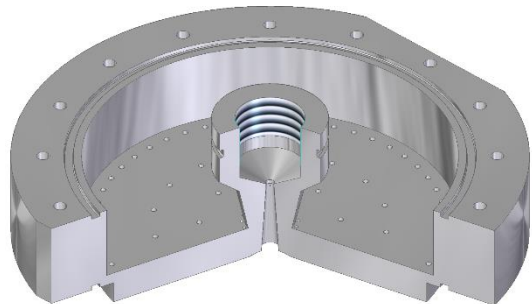


**Fig. 10 Render of Single Part Injector**

The original chamber/nozzle assembly would be turned down to remove the old fuel manifold walls. A flanged piece was added to the chamber/nozzle assembly to externally fasten the injector and fuel manifold cap using larger bolts. This lower flange was necessary, as the original nozzle/chamber assembly was slightly smaller than the bolt pattern for the new fasteners. The pattern was widened from the previous diameter to accommodate a new elastomer seal, which was located away from the inner wall of the combustion chamber. This seal would replace the previous copper gasket between the fuel faceplate. The full engine assembly with cutaway view is shown in Fig. 11.

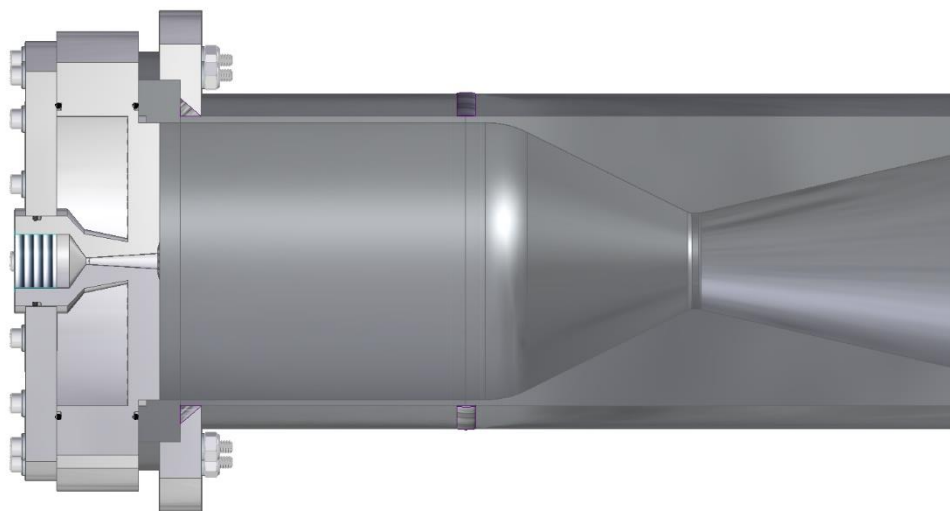


**Fig. 11 Render of Modified Engine Assembly**

#### **D. Propellant Run System**

The loss of the aluminum run tanks was the largest change to the propellant run system. The student-designed and manufactured 1000 psi MAWP tanks were replaced with DOT-rated double ended sample cylinders with a MAWP of 1800 psi. The capacity of the test stand is reduced, but the cylinders were a schedule saving effort. Because the initial static fire was planned to have low propellant load and not attempt a full duration firing of the engine, the acquisition of the cylinders allowed the test campaign preparation to continue while new tanks were designed, procured, manufactured, and tested. Additionally, the DOT rating allowed the cylinders to be used for static fire without a preliminary hydrostatic test, saving even more schedule. A panel had to be developed to support the smaller tanks and the fittings were reworked to accommodate the reduction from 6 outlets to 2 outlets per tank. The redesigned panel is shown in Fig. 9. The run valves and vent valves were also changed from the flight weight servo-ball valves to larger, more reliable pilot operated ball valves. The short duration of the engine firing requires faster valve response, and the nature of an inaugural engine firing requires highly reliable valves. The heavier valves are supported by an aluminum bar connected to the chassis of the fluid panel.

#### **E. Command and Control System**

The command and control system was already undergoing changes up to the critical design review. The decentralized DAQ boxes stationed at the propellant farms and test stand were not effectively using the instrument ports. The test stand had too many instruments to fit in on NI DAQ, while the propellant farms had additional slots. Additionally, the original plan of using LabVIEW to communicate with Arduinos to command valves was causing more reliability and communications issues than direct wiring to the NI DAQ. For this reason, the NI DAQs were centralized to a single box at the field computer and the Arduinos were eliminated. The NI DAQ would command the relays directly. This increased the number of wires running from the field computer to each part of the range, but simplified the architecture and programming, which led to faster and more reliable redlines.

Of course, the purpose of the Arduino was to have logic at the valves capable of safing the system if communications were lost between the field computer and DAQ boxes. The field computer would be handling the entire program, with the ground station remotely monitoring it over fiber optic cable. This setup, instead of having the ground station computer handling the program with the field computer relaying the signal, was selected to improve the efficacy of redlines. However, in the event the signal was lost between the field and ground station visibility to the instrumentation would be lost. A simple system was developed to reliably trigger an abort and ensure the system was safe without instrumentation: a power interrupt. A relay is placed between the field generator and the test stand and receives command voltage from the ground station. If the voltage from the ground station is broken, the power is disconnected from the test stand. A block diagram of the system is shown in Fig. 12.

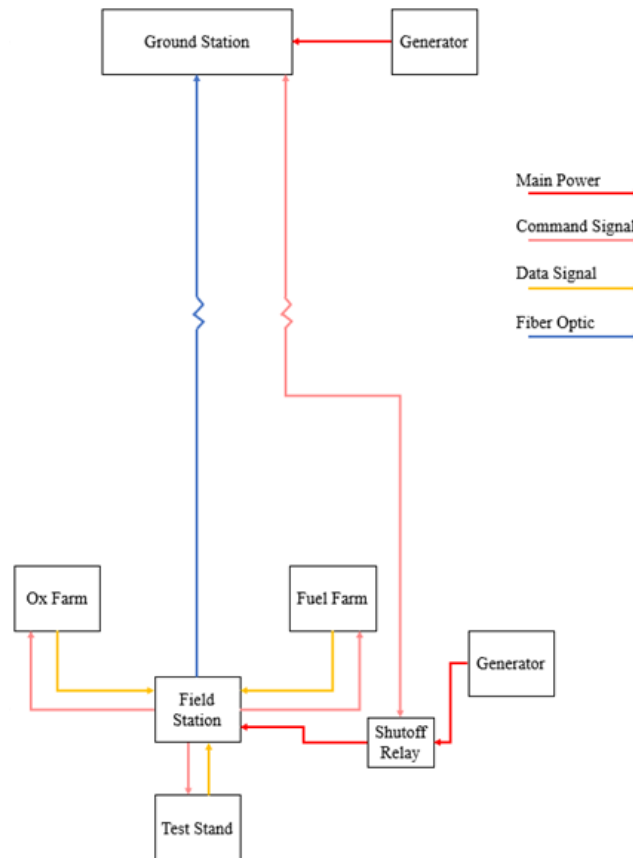


**Fig. 12 Updated Ground System Power and Data Block Diagram**

Every remote operated valve on the system mechanically returns to a safe state upon power loss. While this may be considered an aggressive abort system, it is easy to test and highly reliable.

#### IV. Anomalies and Safety Systems

In addition to functional hardware updates, the safety systems and driving models were also improved upon in the revision of the test stand.

##### A. Blast Calculations

The most energetic anomaly on Tartarus' system is the overpressure of the full load of fuel and oxidizer. This is the release of all pressure energy inside of the tanks without flow restriction. For initial tests, this load is 2 seconds of mass flow. This risk scenario was more likely when the run tanks were student-developed pressure vessels with a shared bulkhead. The team has since transitioned to separate, DOT-rated double ended sample cylinders, but conservatively has chosen to maintain the full overpressure case as the most catastrophic outcome. Using methods

developed by Kashkarov and Molkov, the team performed 2 analyses of the pressure energy. The first is a Brodes energy model for compressed gas, and the second TNT Equivalent model. The models were used to determine a pressure decay curve [1]. The data points of the curves are shown in Fig. 13. FEMA [2] and CDC [3] standards were referenced to define what pressures cause the horizontal damages, and the distance is listed underneath each heading

| Overpressure vs Distance: Both Tanks |             |          |                   |             |             |              |              |
|--------------------------------------|-------------|----------|-------------------|-------------|-------------|--------------|--------------|
|                                      |             | Death    | Total Ear rupture | Lung trauma | Barotrauma  | Glass Breaks | 140 dB Limit |
| alpha                                | 1.8         |          |                   |             |             |              |              |
| Distances [ft]                       |             | 5.221729 | 5.682705          | 9.357398    | 16.86596904 | 286.1390306  | 544.5864     |
| Distances [m]                        |             | 1.591583 | 1.732088          | 2.852135    | 5.140747364 | 87.21517652  | 165.9899     |
| TNT dP [psi]                         |             | 55       | 45                | 15          | 4.9999993   | 0.14999946   | 0.07729      |
| TNT dP [atm]                         |             | 3.742528 | 3.062068          | 1.020689    | 0.340229772 | 0.010206858  | 0.005259     |
| TNT dB                               |             | 205.574  | 203.831           | 194.2885    | 184.7461218 | 154.2885168  | 148.5292     |
| Brode's DP [Pa]                      | 1180033.709 | 89988.04 | 80513.87          | 41787.05    | 19257.09636 | 465.277202   | 199.6102     |
| Brode's DP [psi]                     | 171.1494196 | 13.05166 | 11.67755          | 6.060699    | 2.793005691 | 0.067482753  | 0.028951     |
| Brode's DP [atm]                     | 11.64602723 | 0.888113 | 0.79461           | 0.412406    | 0.190052764 | 0.004591929  | 0.00197      |
| Brode's dB                           | 215.4342315 | 193.08   | 192.1138          | 186.4172    | 179.6881593 | 147.3505787  | 140          |
| Max OP [psi]                         |             | 55       | 45                | 15          | 4.9999993   | 0.14999946   | 0.07729      |
| Threshold [psi]                      |             | 55       | 45                | 15          | 5           | 0.15         |              |

**Fig. 13 Results of Blast Radius Calculations**

The following assumptions were made in this analysis:

- Homogeneous properties
- Atmospheric pressure of 14.7 psia
- No chemical release (no combustion or detonation)
- Instantaneous Release of pressure
- Spherical Blast
- 1.8 Reflectivity Coefficient (80% bounceback from downward firing blast)
- Van der Waals Model
- 1404 in<sup>3</sup> Nitrous Oxide Tank Volume
- 819 in<sup>3</sup> Ethane Tank Volume

### B. Nitrous Oxide Decomposition Modeling

The second most energetic anomaly for the Tartarus system is a decomposition of the nitrous oxide present in the tanks. This decomposition can occur at temperatures as low as 98 °F if contamination is present. This decomposition is exothermic and can result in runaway reactions, leading to dramatic overpressures. In order to properly size the relief device for the nitrous oxide tank, a transient decomposition model was constructed to ensure that the relief device could remove pressure from the system faster than the decomposition could create it, ensuring no permanent hardware damage. This model is based on decomposition rate studies found in Reference 4, with values for activation energies at elevated pressures found in Reference 5. A plot of the pressure and temperature inside the nitrous oxide tank over time can be seen in Fig. 14. The rapid increase in pressure due to the decomposition can be seen up until approximately 10 seconds, when

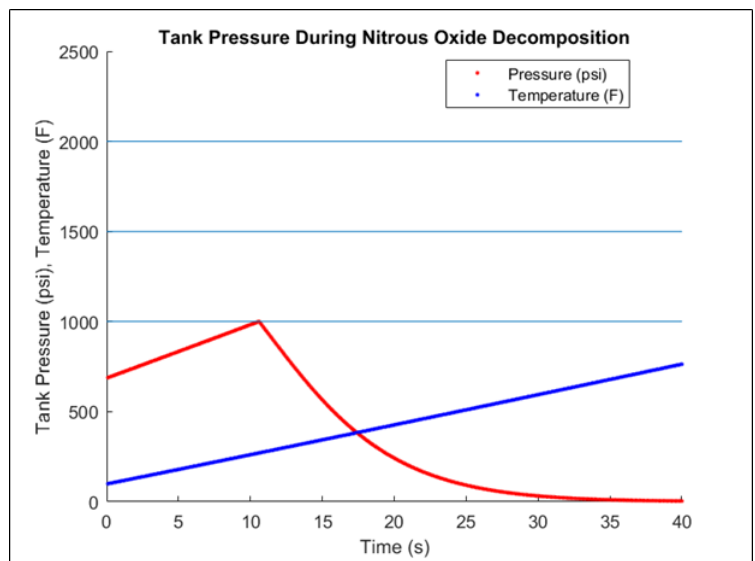


**Fig. 14 Results of Nitrous Oxide Decomposition Model**

the tank pressure reaches 1000 psi and the burst disc ruptures. Then the pressure quickly decreases as the tank vents, ensuring no damage to either the tank or other hardware or instruments.

### C. Personnel Management

While on the test range, operators will wear ANSI Z87.1 compliant protective eyewear, ANSI S3.19-1974 compliant 27 dB noise reduction rating rated hearing protection, long pants, cotton clothing, and closed toed shoes. Steel toed footwear will not be required per OSHA 1910.136(a). Operators will be trained through dry and wet dress rehearsals prior to and on static fire test day. The field team personnel will be required to have at least two operators with active CPR/AED certification. Personnel will be tracked through the use of a badge board at the ground station, where operators must trade their student ID for a numbered neon badge before entering the field. The badge board will be checked prior to entering red (hazardous) steps in the operations. The stand is equipped with a red strobe light to indicate when the stand is in a non-approachable state. The ground station will use a green/yellow/red tower light to indicate if the stand is approachable (green), approachable with test lead approval (yellow), or not approachable (red). The ground station will be protected behind a Kevlar blast curtain and polycarbonate shield. All personnel regardless of role will be required to stand behind these barriers during hazardous (red) operations. The field features multiple safing features for local operators to quickly safe the system, such as switches. The ignition system requires the insertion and turning of a key by the test lead before it can be armed. The ignition system specifically has 4 points, one of which is a physical switch in the field, that must be armed before the ignitor can be fired.

## V. Drivers of Design Updates

The redesign of many parts of the system was gradual as new information was learned or the trade space limitations changed. However, there are 3 identifiable events that drove the most significant change on the system and brought it to its current state.

### A. Critical Design Review

The preliminary design review of the system was in January 2018 and focused on the flight vehicle systems. This review did not cover details of the ground test system. The ground test system had undergone internal maturation and needed a separate review, which took place in October 2019. Preparation for the review forced many loose ends to be addressed and old designs to be reevaluated. When the design was presented, the critiques from experienced industry professionals provided much needed feedback on the more flight-like portions of the test stand that were excessively hazardous. The reviewers offered perspectives and ideas that aren't found in textbooks, which were critical to a young team of undergraduates tackling the problem for the first time. The CDR was also the first formal update to stakeholders in the project in over a year, which opened the door for more mentorship and feedback.

### B. Propellant Tanks Hydrostatic Testing

The aluminum propellant tanks were hydrostatically proof pressure tested shortly after CDR. The goal was to slowly ramp them up to 1500 psi, 1.5x MAWP. The tanks were instrumented with a pressure transducer for the test to detect pressure decay, and the fluid was dyed to detect pinhole leaks. The tanks unfortunately ruptured at roughly 900 psi. The moment of failure is shown in Fig. 15. The failure occurred at the upper bulkhead weld, right down the center of the weld. This failure mode indicates a poor weld quality, not a failure in the heat treatment or design principles of the tank. 6061 aluminum is known to have welding difficulties, and based on sample weld specimens, it is believed that there was contamination within the weld. With limited resources, an in-depth study of the weld cannot be performed. However, better weld specification was added as a lesson learned from the hydrostat. The loss of the tanks primarily drove changes to the run system and the structure of the test stand.



**Fig. 15 Rupture During Hydrostatic Testing**

### C. Integrated Testing

In February and March, the system was undergoing checkouts for static fire. These checkouts included leak checking, low pressure operational checkouts, and high pressure operational checkouts. Many issues with muscle

pressure were experienced and redesigned during this testing. The LabVIEW program was also tested and improved. In addition, the team was better familiarized with the operation of the system, which improved the test procedures.

## **VI. COVID-19 Impact and Future Work**

The engine firing was scheduled for April, with more subscale testing leading up to that date. As a university team, access to facilities was completely restricted when the COVID-19 pandemic policies were put into place in mid-March. As of this writing, access to facilities is still restricted. Unfortunately, progress towards static fire requires access to the hardware for more integrated testing. In the meantime, the team has been teleworking on forward-thinking design efforts, such as replacing the large propellant tanks and improving the LabVIEW code using virtual instruments. Time has also been taken to invest in workforce training in strategic knowledge gap areas, so that the personnel who have not graduated upon return to site can carry the project forward. Moving into the academic year, the team is preparing two different approaches based on the continuing COVID-19 restrictions. With access to hardware, preparations for hotfire will be restarted, and the date for firing will be set for November 21/22, 2020. All proper precautions will be taken to inhibit the spread of COVID-19 using the Space Hardware Club's COVID-19 procedure manual. Assuming operations are to resume, the main restriction upon the team's time in the machine shop is the fact that the University of Alabama in Huntsville is moving to a fully virtual state on November 30<sup>th</sup>, to reduce transmissions from the Thanksgiving holiday break. This shift to virtual learning will likely mean that the university will move students off campus and prohibit any on campus gatherings. Therefore, the firing date would have to be pushed forward, hence the November 21st date, giving the team less time to properly prepare for the firing. However, if the team is unprepared for the firing, the date will move to sometime in the Spring 2021 semester without hesitation. If facility restrictions are levied, the team will continue remote design efforts and education, as well as review and modification of hotfire procedures and plans. This virtual approach will be used in both scenarios as some team members are not returning to campus in the fall due to justified fear of COVID-19. Therefore, assuming the team gets access to the hardware, the team will have simultaneous design and firing efforts ongoing throughout the fall semester. The design team will be the team members who chose to not return to campus, and the firing team will be the team members who chose to return to campus. With this two-pronged approach, the team is prepared to make strong progress no matter what the COVID-19 and hardware access situations are on campus.

## **VII. Conclusion and Lessons Learned**

Designing a test stand is not a simple task. It is a balance of reliability and novel hardware testing, cost savings and safety. Determining the correct scope for novel hardware testing is often aided by previous experience, which is one of the largest challenges facing any young design team. Through knowledge transfer practices, the team's experience over 3 years of development is leveraged to continue improving future designs. The successes and failures of previous designs should be captured in an accessible form for any team that has transient personnel.

Some of the preliminary design features have continued into the current test stand design, while others have swiftly and permanently been changed. Without the engine firing, it's difficult to say if the current test stand will work as designed. There are still plenty of checkouts and integrated testing to be performed. However, significant risk on the system was brought down due to the changes made between 2018 and 2020. The use of flight hardware with lower safety factors for a hazardous test led to significant operation constraints to protect personnel, which drove up the test complexity and time required. Many operational constraints, especially those from the aluminum propellant tanks, have been alleviated through the reselection to proven and/or certified hardware. If flight hardware must be used, such as flight weight pressure vessels, every effort should be made to prove the hardware prior to hazardous test using controlled proof testing. While the system must return to the more flight-like configuration for a future stage firing, there will be more fidelity in the engine design and less risk on the system. For the current testing campaigns, the heavier and reliable system is the best path forward.

## **Acknowledgements**

Thank you to all the members of Tartarus, past and present, as well as the Space Hardware Club at UAH and the University of Alabama in Huntsville. Thank you also to the Alabama Space Grant Consortium for supporting this project since its inception. Finally, thank you to the industry mentors of this team and Dr. Richard Tantarisis, who have helped drive incredible improvements in the past year.

## References

- [1] Molkov, Vladimir, and Sergii Kashkarov. "Blast wave from a high-pressure gas tank rupture in a fire: Stand-alone and under-vehicle hydrogen tanks." *International Journal of Hydrogen Energy* 40.36 (2015): 12581-12603.
- [2] Chipley, M., Kaminskas, M., Lyon, W., Beshlin, D., and Hester, M., "Reference Manual to Mitigate Potential Terrorist Attacks Against Buildings," FEMA 426, December 2003
- [3] Zipf Jr., R. K., and Cashdollar, K. L., "Effects of Blast Pressure on Structures and the Human Body," NIOSH Docket 125, 2007
- [4] Stokes Fishburne, E., Nicholson, J. R., and Edse, R. "Studies on the Decomposition of Nitrous Oxide," U.S Airforce Aerospace Research Lab., Rept. ARL 63-134, Ohio State University, OH, August 1963
- [5] Kalbeck, W. M. and Silepceovich, C. M., "Kinetics of Decomposition of Nitrous Oxide," *Ind. Eng. Chem. Fundam.*, Vol 17, No. 3, 1978